

Theory of light-induced drift of a binary gas mixture in a capillary

V. G. Chernyak and E. A. Vilisova

A. M. Gor'kii Ural State University, 620083 Ekaterinburg, Russia

(Submitted 15 June 1994; resubmitted 18 October 1994)

Zh. Eksp. Teor. Fiz. **107**, 125–139 (January 1995)

The drift of a binary gas mixture in capillaries induced by a resonant light has been studied theoretically. The surface (accommodation) mechanism and bulk (buffer) mechanism of the effect, which are governed respectively by the difference in the accommodation coefficients and the cross sections for the collisions of excited and unexcited particles of the absorbing component have been analyzed. The hydrodynamic, the intermediate, and the Knudsen drift regimes have been examined. The plots of the kinetic coefficients, which characterize the light-induced flows of the components of the mixture, versus the Knudsen number, the ratios of the molecular masses, and the effective diameters of particles of the absorbing and buffer gases have been obtained. © 1995 American Institute of Physics.

1. INTRODUCTION

The phenomenon of light-induced drift (LID) *in bulk*, which was predicted by Gel'mukhanov and Shalagin,¹ can be described as the appearance of a directed flow of gas which absorbs light selectively with respect to the velocities of molecules and which is found in a mixture with a buffer gas. The presence of a buffer gas, whose molecules interact in different ways with the excited and unexcited particles of the absorbing gas, is of fundamental importance for the existence of light-induced drift in bulk. As a result of such interaction, the buffer gas also flows in the direction opposite to the light-induced drift. It follows from the momentum conservation law that in the case of unrestricted gas the hydrodynamic (average-mass) flow of a mixture is generally equal to zero (if light pressure is ignored). The mechanism for light-induced drift in bulk in the case of unrestricted, spatially uniform gas was analyzed in detail by Dykhne and Starostin.²

In the case of a restricted gas mixture a surface light-induced drift occurs as a result of different interactions of excited and unexcited particles of the active component with the boundary between the phases.^{3,4} A so-called *collisional* light-induced drift is also known to exist in a restricted gas for different transport cross sections for collisions of excited and unexcited particles.^{5,6} In each case, the wall changes the total momentum of the gas mixture, stimulating its macroscopic flow. Near the boundary between the phases, there are therefore not only oppositely directed flows of active gas and buffer gas but also a hydrodynamic flow of the entire mixture. However, far from the wall (on the order of ten mean free paths of molecules) its effect on the state of the gas becomes unimportant and, according to the momentum conservation law, there is no hydrodynamic flow of the mixture.

At the qualitative level, an analysis of the contribution to the net effect of light-induced drift in the capillary of each of the three aforementioned mechanisms is fairly straightforward. At a low concentration of the absorbing gas, the collisions between its molecules can be ignored; i.e., the “collision” mechanism is absent. With regard to the other two mechanisms, the contribution from each of them to the light-

induced drift is different, depending on the values of the Knudsen number ($Kn=l/R_0$, where l is the mean free path of molecules in the gas, and R_0 is the radius of the capillary). In the hydrodynamic regime ($Kn \ll 1$), only a few particles of the active gas interact with the surface of the capillary. Specifically, only those particles which are situated in the thin (on the order of l) layer near the wall interact with the surface of the capillary. For $Kn \ll 1$, the bulk (“buffer”) mechanism for light-induced drift is therefore the controlling mechanism. In the intermediate regime ($Kn \approx 1$), a significant contribution from each mechanism is expected. In the free-molecule regime ($Kn \gg 1$), in which there are no collisions between particles of the active gas and the buffer gas, only a light-induced drift at the surface—a directed flow of the absorbing gas—is possible, while the buffer gas is at rest.

Such a picture was observed in the experimental study⁷ of a drift of sodium vapor in an atmosphere of inert gases. It was established that the velocity of light-induced drift is a nonmonotonic function of the buffer gas pressure. The velocity reaches a maximum value in the intermediate regime and then decreases with further decrease of the gas pressure in the capillary.

Experimental studies of light-induced drift in capillaries over a wide range of Knudsen numbers can be reliable sources of information about the transport and accommodation properties of excited particles. An adequate theory must be developed for this purpose.

We have attempted to theoretically study the bulk (buffer) mechanism and surface (accommodation) mechanism for light-induced drift of a binary gas mixture in a capillary for arbitrary Knudsen numbers.

2. STATEMENT OF THE PROBLEM

Let us consider mass transfer in a binary gas mixture which fills a capillary, whose length L is much greater than its radius R_0 . The flow profiles in this case depend solely on the radial coordinate \bar{r} , and end effects can be ignored.

A traveling light wave, which is directed along the z axis of the capillary, is absorbed by the particles of one of the components in the electronic (for atoms) or vibrational–

rotational (for molecules) transition from the ground state n to an excited state m . The frequency ω of the monochromatic light is offset from the center of the absorption line, ω_{mn} , by $\Omega = (\omega - \omega_{mn}) \ll \omega$, ω_{mn} . Because of the Doppler effect, only those particles of the absorbing component whose projection of the velocity \mathbf{v}_1 in the direction of the wave vector \mathbf{k} are close to the resonance value $\mathbf{k}\mathbf{v}_1 = \Omega$ interact with the light. The particles which have absorbed light change their transport properties—in particular, the collision cross section. The gas can therefore be considered a three-component mixture. The particles of the m th and n th components of the absorbing gas in this case have the same masses $m_m = m_n = m_1$ but different effective diameters, $d_n \neq d_m$, and they can undergo mutual transformations due to the radiative decay of an excited level or to stimulated and collision-induced transitions.

The velocity distributions of the excited f_m and unexcited f_n particles of the absorbing gas have a Bennett peak and a dip, respectively, near the resonant velocity,⁸ $v_{1z} = \Omega/k$. At $\Omega \neq 0$, these distributions are asymmetric about $v_{1z} = 0$. There exist therefore oppositely directed macroscopic fluxes of excited J_m and unexcited J_n particles along the capillary. Because the excited and unexcited particles interact differently with the wall and the buffer particles, the partial fluxes J_n and J_m experience different resistances, which gives rise to a net flow of the absorbing component in the capillary, $J_1 = J_m + J_n$ —the light-induced drift, which causes the gas mixture to segregate.

The distribution of the excited f_m and unexcited f_n particles of the active component and the distribution of particles of the buffer gas, f_2 , satisfy the coupled kinetic equations⁸

$$\begin{aligned} \mathbf{v}_1 \nabla f_m &= \frac{1}{2} \kappa(\mathbf{v}) \Gamma_m (f_n - f_m) - \Gamma_m f_m + S_m, \\ \mathbf{v}_1 \nabla f_n &= -\frac{1}{2} \kappa(\mathbf{v}) \Gamma_m (f_n - f_m) + \Gamma_m f_m + S_n, \\ \mathbf{v}_2 \nabla f_2 &= S_2, \end{aligned} \quad (1)$$

where

$$\kappa(\mathbf{v}) = \frac{4|G_{mn}|^2 \Gamma}{\Gamma_m [\Gamma^2 + (\Omega - \mathbf{k}\mathbf{v}_1)^2]}, \quad G_{mn} = \frac{E_0 d_{mn}}{2\hbar};$$

$$S_m = S_{mm} + S_{mn} + S_{m2}, \quad S_n = S_{nm} + S_{nn} + S_{n2},$$

$$S_2 = S_{2m} + S_{2n} + S_{22},$$

Γ_m is the radiative decay constant, Γ is the homogeneous half-width of the absorption line, S_{ij} are the Boltzmann collision integrals between particles of the i th and j th species, E_0 is the electric field amplitude, d_{mn} is the dipole moment of the m - n transition, \hbar is Planck's constant, and $\kappa(\mathbf{v})$ is the saturation parameter, which characterizes the induced transition probability and which is proportional to the radiation intensity I .

We assume that the collisions of gas particles with the capillary wall are elastic, and that they can be approximated by a specular-diffuse Maxwell model, according to which some particles ε_i of i th species, after a collision with the wall, are diffusely scattered with a Maxwellian velocity dis-

tribution, while the remainder $1 - \varepsilon_i$ are specularly reflected. We can then write the boundary conditions for Eqs. (1) as follows:

$$\begin{aligned} f_i^+(\mathbf{v}) &= \varepsilon_i f_i^s(\mathbf{v}) + (1 - \varepsilon_i) f_i^-(\mathbf{v} - 2(\mathbf{v}\mathbf{n})\mathbf{n}), \quad \mathbf{v}\mathbf{n} > 0, \\ f_i^s &= n_i^s \left(\frac{m_i}{2\pi k_B T} \right)^{3/2} \exp\left(-\frac{m_i v^2}{2k_B T}\right), \quad i = m, n, 2. \end{aligned} \quad (2)$$

Here \mathbf{n} is the inner normal to the capillary wall; the superscripts $+$, s , and $-$ denote respectively the reflected particles, the diffuse particles, and the particles incident on the surface; n_i^s is the number density of the diffusely scattered particles of the i th species, m_i is the mass of the particles of the i th species, k_B is the Boltzmann constant, and T is the gas temperature.

Let us consider the case in which the saturation parameter is small, $\kappa(\mathbf{v}) \ll 1$. This imposes a corresponding constraint on the intensity I . The states of the components will then be slightly out of equilibrium and the distribution functions can be written in the form of small perturbations of the Maxwellian distributions:

$$\begin{aligned} f_i &= f_{i0} [1 + h_i(\bar{\mathbf{r}}, \mathbf{v})], \\ f_{i0} &= n_{i0} \left(\frac{m_i}{2\pi k_B T} \right)^{3/2} \exp\left(-\frac{m_i v^2}{2k_B T}\right), \quad i = m, n, 2, \end{aligned} \quad (3)$$

where n_{i0} is the equilibrium number density of the i th component.

Let us assume that particle-particle collisions are elastic. Each collision rate $\gamma_i = \gamma_{ii} + \gamma_{ij} + \gamma_{ik}$ (where γ_{ii} , γ_{ij} , and γ_{ik} are the effective elastic collision rates of particles of the i th species with particles of the i th, j th, and k th species, respectively) in this case is much higher than the radiative decay rate Γ_m ; i.e., $\Gamma_{mi} = \Gamma_m / \gamma_i \ll 1$.

For an optically thin medium, the change in intensity ΔI along the length of the capillary is small, and in first approximation the dependence of the perturbation on the longitudinal coordinate z can be ignored. We assume that the radiation intensity is uniform along the cross section of the capillary. The saturation parameter $\kappa(\mathbf{v})$ in this case does not depend on the radial coordinate \bar{r} , and neither transverse diffusive flow nor light-induced diffusive striction and expulsion of particles by the light field occur.⁹

The assumption that the induced transition probability is low implies that the density of excited particles is much lower than the density of unexcited particles. Let us also consider the case in which the density of buffer particles is much higher than the density of absorbing particles. We thus have $n_m \ll n_n \ll n_2$ and $n_1 = (n_n + n_m) \ll n_2$. The collision integrals S_{mm} , S_{mn} , S_{nm} , and S_{nn} in Eqs. (1) can be ignored in this case. Since collisions between particles of the absorbing gas are disregarded, only two light-induced drift mechanisms—the bulk (buffer) mechanism and the surface mechanism—are important.

The kinetic equations (1), linearized with respect to the perturbations of the distribution functions h_i and with respect to the small parameters $\Gamma_{mi} = \Gamma_m / \gamma_i$, n_m/n_n , n_m/n_2 , and n_n/n_2 , can be put in the form

$$\mathbf{c}_{m\perp} \frac{\partial h_m}{\partial \mathbf{r}} - \frac{n_n}{n_m} R_m \Gamma_{mm} \frac{\kappa(\mathbf{v})}{2} = L_m,$$

$$\mathbf{c}_{n\perp} \frac{\partial h_n}{\partial \mathbf{r}} - R_n \Gamma_{nn} \frac{\kappa(\mathbf{v})}{2} = L_n, \quad \mathbf{c}_{2\perp} \frac{\partial h_2}{\partial \mathbf{r}} = L_2, \quad (4)$$

where

$$\mathbf{c}_i = \frac{\mathbf{v}_i}{\bar{v}_i}, \quad c_{i\perp}^2 = c_{ir}^2 + c_{i\varphi}^2, \quad \bar{v}_i = \sqrt{\frac{2k_B T}{m_i}},$$

$$\mathbf{r} = \frac{\tilde{\mathbf{r}}}{R_0}, \quad R_i = \frac{R_0 \gamma_{i2}}{\bar{v}_i}, \quad i = n, m, 2.$$

Here $\mathbf{c}_{i\perp}$ is the vector component of the dimensionless velocity of the particles of i th species along the cross section of the capillary.

We will use second approximations of the linearized elastic-collision integrals L_i .¹⁰ Retaining only the odd terms in the velocity c_z (only these terms determine the gas flow) and disregarding such a subtle effect as the isothermal heat transfer, we can write these approximations as follows:

$$L_i = R_i \left[-h_i + 2c_{iz} (1 - \varphi_{i2}^{(1)}) u_i + 4c_{ir} c_{iz} \right. \\ \left. \times (1 - \varphi_{i2}^{(3)}) \pi_{irz} \right], \quad i = n, m,$$

$$L_2 = R_2 \left[-h_2 + 2c_{2z} \left\{ u_2 + \sqrt{\frac{m_1}{m_2}} \left(\frac{n_m}{n_2} \psi_{m2}^{(1)} u_m \right. \right. \right. \\ \left. \left. + \frac{n_n}{n_2} \psi_{n2}^{(1)} u_n \right) \right\} + 4c_{2r} c_{2z} \left\{ (1 - \psi_{22}^{(3)} + \psi_{22}^{(4)}) \pi_{2rz} \right. \\ \left. \left. + \frac{n_m}{n_2} \psi_{m2}^{(4)} \pi_{mrz} + \frac{n_n}{n_2} \psi_{n2}^{(4)} \pi_{nrz} \right\} \right], \quad (5)$$

where

$$\varphi_{i2}^{(k)} = \frac{v_{i2}^{(k)}}{\gamma_{i2}}, \quad \psi_{i2}^{(k)} = \frac{v_{i2}^{(k)}}{\gamma_{22}},$$

$$u_i = \frac{U_i}{\bar{v}_i} = \int c_{iz} E_i h_i d\mathbf{c}_i, \quad \pi_{irz} = \frac{P_{irz}}{2p_i}$$

$$= \int c_{ir} c_{iz} E_i h_i d\mathbf{c}_i,$$

$$E_i = \pi^{-3/2} \exp(-c_i^2), \quad i = m, n, 2. \quad (6)$$

Here U_i , P_{irz} , and p_i are the partial velocity, the stress tensor, and the pressure of the i th component, respectively. The expressions for the frequencies $v_{i2}^{(k)}$ in terms of the particle masses and the Chapman–Cowling Ω integrals are given in Ref. 10. The rarefaction parameter R_i is inversely proportional to the Knudsen number [see expression (15)].

We note that kinetic equations (4) for the excited and unexcited components of the absorbing gas do not depend on each other or on the equation for the buffer gas. On the other hand, the last expression in (4) in terms of the collision integral L_2 includes the characteristics of each component of the absorbing gas. The distribution function of the buffer particles can therefore be determined only after solving the first two equations of the system (4). Such a substantial

mathematical simplification is the result of an assumption that the concentration of the absorbing gas is low.

The linearized boundary conditions (2) for the perturbation functions h_i have the form

$$h_i^+(\mathbf{r}_0, \mathbf{c}) = (1 - \varepsilon_i) h_i^-(\mathbf{r}_0, \mathbf{c}) + \varepsilon_i \frac{n_i^s - n_{i0}}{n_{i0}},$$

$$\mathbf{r}_0 = \frac{\tilde{\mathbf{r}}_0}{R_0}, \quad |\mathbf{r}_0| = 1, \quad i = m, n, 2. \quad (7)$$

The second term on the right side of the expression for h_i^+ in (7) does not depend on the molecular velocities, and therefore does not contribute to the macroscopic velocity or the stress tensor [Eq. (6)]. We will therefore omit it below.

Equations (4)–(7) can be used to uniquely determine the functions $h_i(\mathbf{r}, \mathbf{c})$, where $i = m, n, 2$. We feel, however, that it would ultimately be worthwhile to consider the resulting flows of the absorbing gas J_1 and the buffer gas J_2 , averaged over the cross section of the capillary:

$$J_1 = J_m + J_n = 2\bar{v}_1 \int_0^1 (n_n u_n + n_m u_m) r dr,$$

$$J_2 = 2\bar{v}_2 \int_0^1 n_2 u_2 r dr. \quad (8)$$

Here $J = J_1 + J_2$ is the average flow of the gas mixture.

For the numerical calculations it is convenient to use the dimensionless quantities G_1 and G_2 , which are related to the flows J_1 and J_2 by

$$J_i = \frac{n_i R_0 \Gamma_m}{2\pi} \kappa G_i, \quad i = 1, 2, \quad (9)$$

where

$$\kappa = \int_{-\infty}^{\infty} c_{1z} \exp(-c_{1z}^2) \kappa(\mathbf{v}) d\mathbf{c}_{1z}.$$

Here $n_1 = n_m + n_n$ is the particle concentration of the absorbing gas.

For any parameter values $\Gamma/(k\bar{v}_1)$ and $\Omega/(k\bar{v}_1)$, the value of κ can be expressed in terms of the plasma function.¹¹ In the case of inhomogeneous broadening ($\Gamma \ll k\bar{v}_1$) and homogeneous broadening ($\Gamma \gg k\bar{v}_1$) the value of κ is

$$\kappa = \begin{cases} \frac{4\Omega\sqrt{\pi}}{\Gamma_m} \left(\frac{|G_{mn}|}{k\bar{v}_1} \right)^2, & (|\Omega|, \Gamma) \ll k\bar{v}_1, \\ \frac{4k\bar{v}_1\Omega\Gamma}{\Gamma_m} \left(\frac{|G_{mn}|}{\Omega^2 + \Gamma^2} \right)^2, & (|\Omega|, \Gamma) \gg k\bar{v}_1. \end{cases}$$

3. SOLUTION OF THE KINETIC EQUATIONS

We will use the integral–moment method based on the transformation of the integrodifferential kinetic equation for the distribution function to a system of integral equations for its moments.

Using the boundary conditions (7), we integrate each of the kinetic equations in (4) in the direction of the velocity vector $\mathbf{c}_{i\perp}$ (Fig. 1).¹² Using the expressions for the perturbation functions h_i which we obtained and the definitions (6) for macroscopic quantities, we obtain the following three

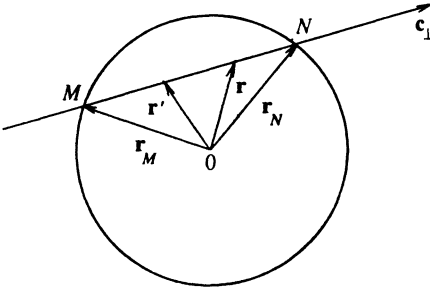


FIG. 1. Diagram of the integration in the direction of c_1 .

systems of integral equations for dimensionless velocities u_i and stress tensors π_{irz} of the absorbing component ($i = m, n$) and the buffer component ($i = 2$) of the gas mixture:

1. For the absorbing gas we have $i = m, n$.

$$u_i = \frac{R_i}{\pi} \int_{\Sigma} \left[\frac{A\kappa D_i}{\sqrt{\pi} R_i} \left(\frac{T_0}{|\mathbf{r}-\mathbf{r}'|} - \frac{K_{0i}}{|\mathbf{r}_N-\mathbf{r}'|} \right) + (1 - \varphi_{i2}^{(1)}) u_i \left(\frac{T_0}{|\mathbf{r}-\mathbf{r}'|} - \frac{K_{0i}}{|\mathbf{r}_N-\mathbf{r}'|} \right) + 2(1 - \varphi_{i2}^{(3)}) \pi_{irz} \left(\frac{T_1 \mathbf{e}}{|\mathbf{r}-\mathbf{r}'|} - \frac{K_{1i} \mathbf{e}_0}{|\mathbf{r}_N-\mathbf{r}'|} \right) \frac{\mathbf{r}'}{r'} \right] d\mathbf{r}', \quad (10)$$

$$\pi_{irz} = \frac{R_i}{\pi} \int_{\Sigma} \left[\frac{A\kappa D_i}{\sqrt{\pi} R_i} \left(\frac{T_1}{|\mathbf{r}-\mathbf{r}'|} - \frac{K_{1i}}{|\mathbf{r}_N-\mathbf{r}'|} \right) + (1 - \varphi_{i2}^{(1)}) u_i \left(\frac{T_1}{|\mathbf{r}-\mathbf{r}'|} - \frac{K_{1i}}{|\mathbf{r}_N-\mathbf{r}'|} \right) + 2(1 - \varphi_{i2}^{(3)}) \pi_{irz} \left(\frac{T_2 \mathbf{e}}{|\mathbf{r}-\mathbf{r}'|} - \frac{K_{2i} \mathbf{e}_0}{|\mathbf{r}_N-\mathbf{r}'|} \right) \frac{\mathbf{r}'}{r'} \right] d\mathbf{r}'. \quad (11)$$

2. For the buffer gas we have

$$u_2 = \frac{R_2}{\pi} \int_{\Sigma} \left\{ \left[u_2 + \sqrt{\frac{m_1}{m_2}} \left(\frac{n_m}{n_2} \psi_{m2}^{(1)} u_m + \frac{n_n}{n_2} \psi_{n2}^{(1)} u_n \right) \right] \times \left(\frac{T_0}{|\mathbf{r}-\mathbf{r}'|} - \frac{K_{02}}{|\mathbf{r}_N-\mathbf{r}'|} \right) + 2 \left[(1 - \psi_{22}^{(3)} + \psi_{22}^{(4)}) \pi_{2rz} + \frac{n_m}{n_2} \psi_{m2}^{(4)} \pi_{mrz} + \frac{n_n}{n_2} \psi_{n2}^{(4)} \pi_{nrz} \right] \left(\frac{T_1 \mathbf{e}}{|\mathbf{r}-\mathbf{r}'|} - \frac{K_{12} \mathbf{e}_0}{|\mathbf{r}_N-\mathbf{r}'|} \right) \frac{\mathbf{r}'}{r'} \right\} d\mathbf{r}', \quad (12)$$

$$\pi_{2rz} = \frac{R_2}{\pi} \int_{\Sigma} \left\{ \left[u_2 + \sqrt{\frac{m_1}{m_2}} \left(\frac{n_m}{n_2} \psi_{m2}^{(1)} u_m + \frac{n_n}{n_2} \psi_{n2}^{(1)} u_n \right) \right] \times \left(\frac{T_1}{|\mathbf{r}-\mathbf{r}'|} - \frac{K_{12}}{|\mathbf{r}_N-\mathbf{r}'|} \right) + 2 \left[(1 - \psi_{22}^{(3)} + \psi_{22}^{(4)}) \pi_{2rz} \right. \right.$$

$$\left. + \frac{n_m}{n_2} \psi_{m2}^{(4)} \pi_{mrz} + \frac{n_n}{n_2} \psi_{n2}^{(4)} \pi_{nrz} \right] \left(\frac{T_2 \mathbf{e}}{|\mathbf{r}-\mathbf{r}'|} - \frac{K_{22} \mathbf{e}_0}{|\mathbf{r}_N-\mathbf{r}'|} \right) \frac{\mathbf{r}'}{r'} \right\} \frac{\mathbf{e} \mathbf{r}}{r} d\mathbf{r}', \quad (13)$$

where

$$\mathbf{e} = \frac{\mathbf{r}-\mathbf{r}'}{|\mathbf{r}-\mathbf{r}'|}, \quad \mathbf{e}_0 = \frac{\mathbf{r}_N-\mathbf{r}'}{|\mathbf{r}_N-\mathbf{r}'|}, \quad A = \frac{\tilde{r}_0 \Gamma_m}{2\tilde{v}_1},$$

$$D_i = \begin{cases} n_n/n_m, & i = m \\ -1, & i = n \end{cases},$$

$$T_p(t) = \int_0^\infty x^p \exp(-x^2 - t/x) dx,$$

$$K_{pi} = \frac{\mathbf{r}_M \mathbf{r}}{r^2} \sum_{k=1}^{\infty} (1 - \varepsilon_i)^k T_p [R_i ((k-1) |\mathbf{r}_N - \mathbf{r}_M| + |\mathbf{r} - \mathbf{r}_M| + |\mathbf{r}_N - \mathbf{r}'|)], \quad i = m, n, 2.$$

The argument t of the functions T_p in Eqs. (10) and (11) is $t = R_i |\mathbf{r}-\mathbf{r}'|$, and the argument t in Eqs. (12) and (13) is $t = R_2 |\mathbf{r}-\mathbf{r}'|$. The integration in (10)–(13) is over the cross-sectional area of the capillary, Σ .

Equations (10)–(13) are Fredholm integral equations of the second kind. For the solution of these equations it is convenient to use the Bubnov–Galerkin method,¹³ since it allows us to calculate the coordinate-averaged flows J_1 and J_2 , without calculating the velocity u_i and stress π_{irz} profiles ($i = n, m, 2$). The convergence rate of the method depends on the choice of the approximating expression for the macroscopic parameters. The experimental study of Chernyak and coworkers¹² has shown that approximations of the type

$$\tilde{u}_i = a_{1i} + a_{2i} r^2, \quad \tilde{\pi}_{irz} = a_{3i} r, \quad i = n, m, 2 \quad (14)$$

provide sufficiently accurate results (within an error of $\approx 3\%$) for the fluxes of absorbing and buffer particles over the entire range of Knudsen numbers.

Substituting relations (14) in the integral equations (10)–(13) and requiring that the expressions which we obtained be orthogonal to each basis function [1 and r^2 for (10) and (12), r for (11) and (13)], we obtain a system of linear algebraic equations for the unknowns a_{1i} , a_{2i} , and a_{3i} . The orthogonality condition of the two arbitrary functions f and g has the form

$$2\pi \int_0^1 f(r)g(r)r dr = 0.$$

We choose the effective collision rate γ_{i2} in the form $\gamma_{i2} = \nu_{i2}^{(1)}$, where $i = m, n$, and we choose the rate γ_{22} in the form $\gamma_{22} = \nu_{22}^{(3)} - \nu_{22}^{(4)}$, by analogy with the Bhatnagar–Gross–Krook model for a one-component gas. The gas particles are modeled as elastic, rigid spheres with diameters d_m , d_n , and d_2 for the excited, unexcited, and buffer particles, respectively. The rarefaction parameter R_n can then be related to the Knudsen number:

$$R \equiv R_n = \frac{8}{3\sqrt{\pi}} \left(\frac{m_2}{m_1 + m_2} \right) \frac{1}{Kn}, \quad Kn = \frac{l_n}{R_0},$$

$$l_n = \frac{1}{\pi n_2 d_{n2}} \sqrt{\frac{m_2}{m_1 + m_2}}, \quad \frac{R_m}{R} = \left(\frac{d_{m2}}{d_{n2}} \right)^2,$$

$$\frac{R_2}{R} = \frac{3}{5} \left(\frac{d_2}{d_{n2}} \right)^2 \sqrt{\frac{2(m_1 + m_2)}{m_2}}, \quad d_{i2} = \frac{1}{2} (d_i + d_2),$$

$$i = m, n, \quad (15)$$

where l_n is the mean free path of the unexcited particles of the absorbing gas.

To reduce the number of adjustable parameters and to simplify the numerical calculations, we restrict the analysis to an approximation in which the difference between the diameters of the excited and unexcited particles is small and we assume that the scattering of particles at the capillary wall is nearly diffuse. As a result, we introduce the small parameters

$$\frac{|\Delta d|}{d_{n2}} \ll 1, \quad 1 - \varepsilon_i \ll 1, \quad i = m, n, 2,$$

$$\Delta d = d_m - d_n. \quad (16)$$

Linearizing expression (9) with respect to the parameters (16) for the flow of the absorbing gas (light-induced drift), we obtain

$$J_1 = \frac{n_1 R_0 \Gamma_m \kappa}{2\sqrt{\pi}} \left(G_1^{(1)} \Delta \varepsilon + G_1^{(2)} \frac{\Delta d}{d_{n2}} \right), \quad \Delta \varepsilon = \varepsilon_n - \varepsilon_m, \quad (17)$$

where

$$G_1^{(1)} = A_1 - \frac{\Phi}{\pi(\pi/2 + \Phi D)} \left(B_1 - \frac{C_1 \Phi}{\pi/2 + \Phi D} \right), \quad (18)$$

$$G_1^{(2)} = A_2 - \frac{\Phi}{\pi(\pi/2 + \Phi D)} \left(B_2 - \frac{C_2 \Phi}{\pi/2 + \Phi D} \right),$$

$$\Phi = \frac{4}{5} \frac{m_2}{m_1 + m_2} - 1. \quad (19)$$

The dependence of the kinetic coefficients $G_1^{(1)}$ and $G_1^{(2)}$ on the molecular masses is determined totally by the factor Φ . The quantities $A_1, A_2, B_1, B_2, C_1, C_2$, and D depend solely on the rarefaction parameter R .

In a similar way, we obtain the following expression for the flow of buffer gas:

$$J_2 = \frac{n_1 R_0 \Gamma_m \kappa}{2\sqrt{\pi}} \left(G_2^{(1)} \Delta \varepsilon + G_2^{(2)} \frac{\Delta d}{d_{n2}} \right). \quad (20)$$

The kinetic coefficients $G_2^{(1)}$ and $G_2^{(2)}$ depend on the rarefaction parameter R and on the ratio of the masses m_1/m_2 and the diameters d_n/d_2 of the particles of the absorbing gas and the buffer gas.

The average flow of the gas mixture is given by the expressions

$$J = J_1 + J_2 = \frac{n_1 R_0 \Gamma_m \kappa}{2\sqrt{\pi}} \left(G^{(1)} \Delta \varepsilon + G^{(2)} \frac{\Delta d}{d_{n2}} \right),$$

$$G^{(1)} = G_1^{(1)} + G_2^{(1)}, \quad G^{(2)} = G_1^{(2)} + G_2^{(2)}. \quad (21)$$

The absorbing and buffer gas flows and the flow of the mixture as a whole are therefore determined, as can be seen from relations (17), (20), and (21), by the kinetic coefficients $G_1^{(1)}, G_2^{(1)}, G_1^{(2)}, G_2^{(2)}, G^{(1)}$, and $G^{(2)}$ which characterize the surface mechanism and the bulk mechanism of these flows.

The error in the numerical calculations of the Galerkin coefficients for determination of the constants a_{1i}, a_{2i} , and a_{3i} in relations (14) does not exceed 0.1% for all the given parameter values.

The analytic expressions for the kinetic coefficients $G_1^{(1)}, G_1^{(2)}, G_2^{(1)}$, and $G_2^{(2)}$ were obtained only for large and small values of the Knudsen number.

1. An almost free-molecule regime ($Kn \gg 1$ or $R \ll 1$):

The quantities contained in expressions (18) and (19) have, up to terms of order R , the form

$$A_1 = 3.009 + 6R \ln R + 3.24R + \dots,$$

$$A_2 = R \ln R + 0.616R + \dots,$$

$$B_1 = O(R^2), \quad B_2 = 1.234R + \dots,$$

$$C_1 = O(R^4), \quad C_2 = O(R^3), \quad D = O(R^2).$$

For the kinetic coefficients which characterize the flow of absorbing gas we then obtain

$$G_1^{(1)} = 3.009 + 6R \ln R + 3.24R + \dots, \quad (22)$$

$$G_1^{(2)} = R \ln R + (0.616 - 0.25\Phi)R + \dots \quad (23)$$

The expressions for the kinetic coefficients which characterize the buffer gas flow have, up to terms of order $R^2 \ln R$, the form

$$G_2^{(1)} = \Phi_1 [4.527R + (9.027 + 10.213\Phi_2)R^2 \ln R] + \dots, \quad (24)$$

$$G_2^{(2)} = [\Phi_1(2.264 - 0.239\Phi) - 0.2\Phi_3]R + \Phi_1 [3.009 + (5.106 - 0.54\Phi)\Phi_2]R^2 \ln R + \dots, \quad (25)$$

where

$$\Phi_1 = \sqrt{\frac{m_1}{m_2}}, \quad \Phi_2 = \frac{\sqrt{1 + m_1/m_2}}{(1 + d_n/d_2)^2},$$

$$\Phi_3 = \frac{m_1}{m_1 + m_2}.$$

2. Hydrodynamic regime with slipping ($Kn \ll 1$ or $R \gg 1$):

The quantities contained in expressions (18) and (19) have, up to terms of order R^{-2} , the form

$$A_1 = \frac{1}{\sqrt{\pi R^2}} + \dots, \quad A_2 = -\frac{1}{R} + \frac{2}{\sqrt{\pi R^2}} + \dots,$$

$$B_1 = O(R^{-3}), \quad B_2 = O(R^{-3}), \quad C_1 = O(R^{-4}),$$

$$C_2 = O(R^{-4}), \quad D = -\frac{\pi}{2} + \frac{2\pi^{1/2}}{R} + \dots$$

TABLE I. The quantities $A_1, A_2, B_1, B_2, C_1, C_2$, and D contained in Eqs. (18) and (19).

R	A_1	$-B_1 \cdot 10^2$	$-C_1 \cdot 10^3$	$-D$	$-A_2 \cdot 10^1$	$B_2 \cdot 10^2$	$-C_2 \cdot 10^2$
0.01	2.76	$7.14 \cdot 10^{-2}$	$1.57 \cdot 10^{-5}$	$5.17 \cdot 10^{-5}$	$4.01 \cdot 10^{-1}$	1.16	$1.23 \cdot 10^{-4}$
0.04	2.35	$9.22 \cdot 10^{-1}$	$3.10 \cdot 10^{-9}$	$7.96 \cdot 10^{-4}$	1.07	3.88	$6.79 \cdot 10^{-3}$
0.07	2.07	2.37	$2.33 \cdot 10^{-2}$	$2.35 \cdot 10^{-3}$	1.50	5.71	$3.17 \cdot 10^{-2}$
0.1	1.85	4.14	$7.96 \cdot 10^{-2}$	$4.63 \cdot 10^{-3}$	1.83	6.87	$8.12 \cdot 10^{-2}$
0.4	$8.59 \cdot 10^{-1}$	2.08·10	4.40	$5.50 \cdot 10^{-2}$	3.11	3.62	1.70
0.7	$5.03 \cdot 10^{-1}$	2.69·10	1.27·10	$1.32 \cdot 10^{-1}$	3.33	-3.91	3.64
1	$3.28 \cdot 10^{-1}$	2.67·10	1.94·10	$2.16 \cdot 10^{-1}$	3.25	-8.71	4.73
2	$1.17 \cdot 10^{-1}$	1.69·10	2.24·10	$4.82 \cdot 10^{-1}$	2.69	-1.13·10	4.25
3	$5.75 \cdot 10^{-2}$	9.65	1.52·10	$6.86 \cdot 10^{-1}$	2.20	-8.39	2.60
4	$3.36 \cdot 10^{-2}$	5.76	9.43	$8.37 \cdot 10^{-1}$	1.83	-5.78	1.50
5	$2.19 \cdot 10^{-2}$	3.64	5.85	$9.49 \cdot 10^{-1}$	1.56	-3.99	$8.85 \cdot 10^{-1}$
6	$1.54 \cdot 10^{-2}$	2.42	3.72	1.03	1.36	-2.82	$5.41 \cdot 10^{-1}$
7	$1.14 \cdot 10^{-2}$	1.68	2.44	1.10	1.20	-2.04	$3.44 \cdot 10^{-1}$
10	$5.60 \cdot 10^{-3}$	$6.84 \cdot 10^{-1}$	$8.30 \cdot 10^{-1}$	1.23	$8.88 \cdot 10^{-1}$	$-8.94 \cdot 10^{-1}$	$1.09 \cdot 10^{-1}$
50	$2.26 \cdot 10^{-4}$	$7.37 \cdot 10^{-3}$	$2.43 \cdot 10^{-3}$	1.50	$1.95 \cdot 10^{-1}$	$-1.08 \cdot 10^{-2}$	$2.60 \cdot 10^{-4}$

For the kinetic coefficients which characterize the absorbing gas flow we then obtain

$$G_1^{(1)} = \frac{1}{\sqrt{\pi R^2}} + \dots, \quad (26)$$

$$G_1^{(2)} = -\frac{1}{R} + \frac{2}{\sqrt{\pi R^2}} + \dots \quad (27)$$

We note that the expression $G_1^{(2)} = -2/R$ was obtained in Ref. 2. The difference by a factor of 2 from the first term on the right-hand side of Eq. (27) is attributable to the fact that an approximation of a spatially homogeneous gas was used in Ref. 2.

For kinetic coefficients which characterize a buffer gas flow we have, for $R \gg 1$,

$$G_2^{(1)} = \left[\Phi_1 \left(\frac{1}{2\sqrt{\pi}} + 3\sqrt{2}\Phi_4 \right) + \Phi_5 \right] \frac{1}{R} + \dots, \quad (28)$$

$$G_2^{(2)} = \left[\Phi_1 \left(\frac{1}{2} + 6\sqrt{2}\Phi_4 \right) + \Phi_5 \right] \frac{1}{R} + \dots, \quad (29)$$

where

$$\Phi_4 = \frac{(1 + m_1/m_2)^{3/2}}{(3 + 5m_1/m_2)(1 + d_n/d_2)^2}, \quad \Phi_5 = \frac{m_1/m_2}{3 + 5m_1/m_2}.$$

The results of numerical calculations of the quantities $A_1, A_2, B_1, B_2, C_1, C_2$ and D for intermediate Knudsen numbers are presented in Table I. The magnitude of the absorbing gas flow for intermediate Knudsen numbers can be determined from Eqs. (18) and (19) for any molecular mass ratio m_1/m_2 .

4. DISCUSSION OF THE RESULTS

Figures 2a and 2b show the plots of the kinetic coefficients $G_1^{(1)}$ and $G_1^{(2)}$, which characterize the surface mechanism and the mechanism for the light-induced drift in bulk,

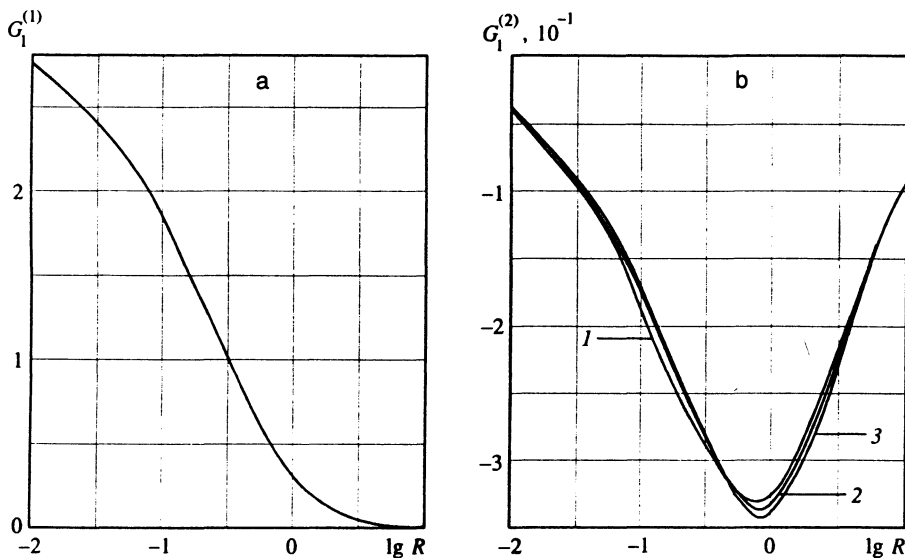


FIG. 2. Plots of the kinetic coefficients $G_1^{(1)}$ (a) and $G_1^{(2)}$ (b) versus the rarefaction parameter R . 1— $m_1/m_2 \ll 1$; 2— $m_1/m_2 \gg 1$; 3— $m_1/m_2 \approx 1$.

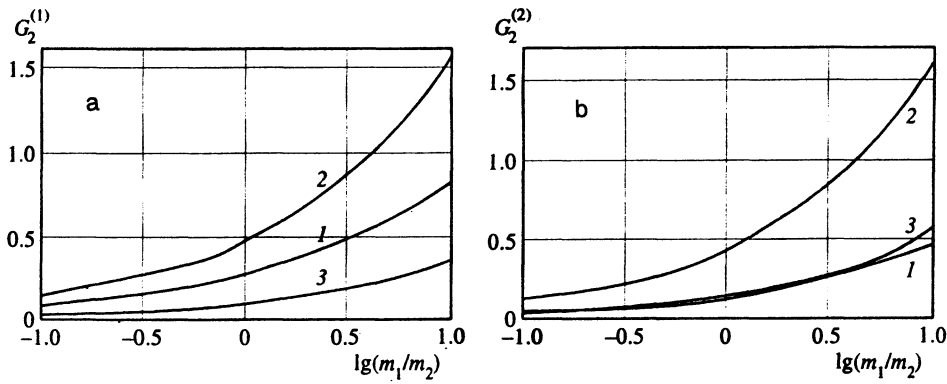


FIG. 3. Plots of the kinetic coefficients $G_2^{(1)}$ (a) and $G_2^{(2)}$ (b) versus m_1/m_2 for $d_1/d_2=1$. 1— $R=0.1$; 2— $R=1$; 3— $R=10$.

plotted as a function of the rarefaction parameter R for three molecular mass ratios $m_1/m_2 \ll 1$, $m_1/m_2 \gg 1$, and $m_1/m_2 \approx 1$. We see that $G_1^{(1)}$ and $G_1^{(2)}$ depend weakly on the molecular mass ratio only in the intermediate regime ($R \approx 1$). The dependence of LID on the molecular mass manifests itself principally in terms of the rarefaction parameter R [see Eq. (15)].

The kinetic coefficients which characterize the flow of buffer gas depend strongly on the molecular mass ratio m_1/m_2 and on the diameters d_1/d_2 . These dependences are illustrated in Figs. 3 and 4. The flow of buffer gas decreases as its molecular weight increases. The Lorentz gas-mixture model is realized in the limit $m_2 \gg m_1$: a small admixture of a light, absorbing gas diffuses through the heavy, stationary buffer gas.

We note that the dependence of the kinetic coefficients $G_2^{(1)}$ and $G_2^{(2)}$ on the diameter ratio d_n/d_2 of the particles of the absorbing and buffer gases is determined by the gas flow regime (Figs. 4a and 4b). While in a nearly free-molecule regime at $R > 1$ $G_2^{(1)}$ and $G_2^{(2)}$ increase only slightly with increasing parameter d_n/d_2 , they actually decrease in the intermediate and hydrodynamic regimes at $R \geq 1$.

In the particular case of a Na-He gas mixture (absorbing gas—sodium vapor, buffer gas—helium), we constructed curves for the kinetic coefficients $G_1^{(1)}$, $G_2^{(1)}$, $G^{(1)} = G_1^{(1)} + G_2^{(1)}$ and $G_1^{(2)}$, $G_2^{(2)}$, $G^{(2)} = G_1^{(2)} + G_2^{(2)}$ versus the rarefaction parameter R . These curves are shown in Fig. 5.

The directions of the surface components of the J_1 and J_2 streams are determined by the difference in the accommo-

dation coefficients of the unexcited and excited particles of the absorbing gas $\Delta\varepsilon = \varepsilon_n - \varepsilon_m$ and the offset between the radiation frequency and the center of the absorption line, $\Omega = \omega - \omega_{mn}$. If $\Delta\varepsilon > 0$, the directions of the surface flow components of the absorbing and buffer gases at $\Omega > 0$ coincide with the direction of radiation, but at $\Omega < 0$ they are opposite the direction of radiation. The fact that the surface components of J_1 and J_2 have the same direction is consistent with momentum conservation in the interaction of the gas with the wall.

The directions of the bulk components of J_1 and J_2 are determined by the difference in the diameters of the excited and unexcited particles of the absorbing gas, Δd , and the offset Ω . If $\Delta d > 0$, the direction of the bulk component of the absorbing gas flow at $\Omega < 0$ is the same as the direction of radiation, but the direction of the bulk component of the buffer gas in the case of collisions between molecules is opposite the direction of radiation, consistent with the momentum conservation law. At $\Omega > 0$, the two gas flows reverse directions.

We see in Fig. 5a that upon transition from free-molecule regime to hydrodynamic regime the value of $G_1^{(1)}$, which characterizes the surface component of the absorbing gas flow, decreases monotonically. Such a dependence is attributable to the fact that the relative number of particles that collide with the capillary walls decreases with increasing rarefaction parameter R , which decreases the importance of the walls as a buffer, causing $G_1^{(1)}$ to decrease.

The kinetic coefficient $G_2^{(1)}$, which characterizes the sur-

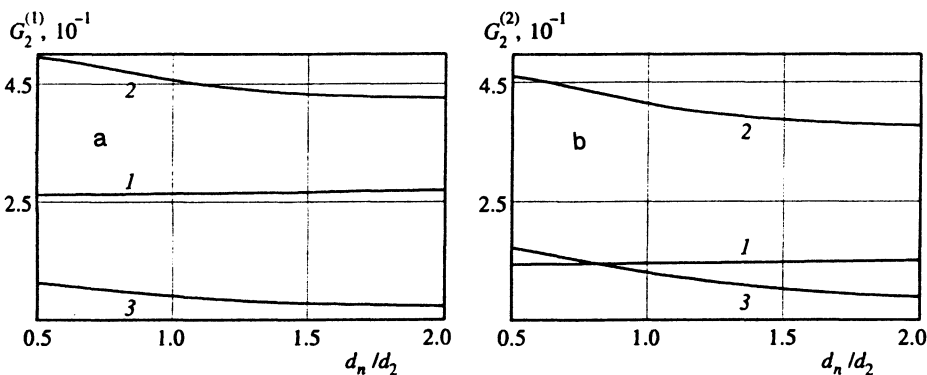


FIG. 4. Plots of the kinetic coefficients $G_2^{(1)}$ (a) and $G_2^{(2)}$ (b) versus d_n/d_2 for $m_1/m_2=1$. 1— $R=0.1$; 2— $R=1$; 3— $R=10$.

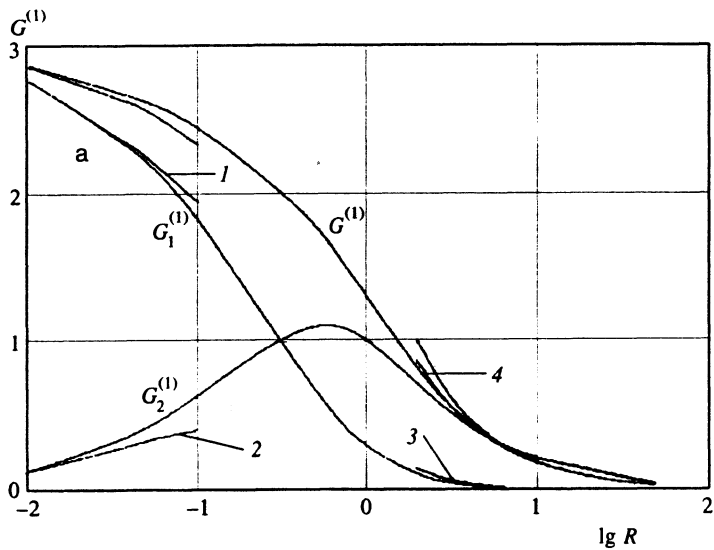
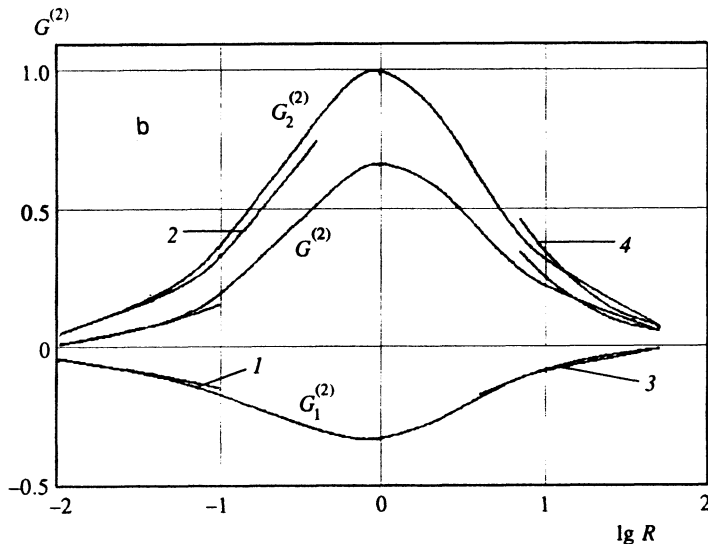


FIG. 5. Plots of the kinetic coefficients $G_1^{(1)}$, $G_2^{(1)}$, $G^{(1)}$ (a) and $G_1^{(2)}$, $G_2^{(2)}$, $G^{(2)}$ (b) versus the rarefaction parameter R for the gas mixture Na-He. 1—Eqs. (22) and (23); 2—Eqs. (24) and (25); 3—Eqs. (26) and (27); 4—Eqs. (28) and (29).



face component of the buffer gas flow, depends nonmonotonically on R . In the transition from the hydrodynamic regime to the intermediate regime (up to the value of $R \approx 0.5$), the increasing flow of the absorbing gas (of its surface component) drags an increasing amount of the buffer gas because of the collision of molecules. However, a further decrease of pressure in the capillary (at $R \leq 0.5$) decreases the number of collisions between molecules, and hence reduces the drag. In the free-molecule regime the buffer gas is stationary.

The kinetic coefficient $G_1^{(2)}$, which characterizes the bulk component of the absorbing gas flow, also depends nonmonotonically on the rarefaction parameter R . In this case $G_1^{(2)} < 0$ (Figs. 5a). For $R \approx 0.8$, this dependence has a minimum (the absolute LID is at a maximum), but in the hydrodynamic ($R \rightarrow \infty$) and the free-molecule ($R \rightarrow 0$) limits $G_1^{(2)} = 0$; i.e., there is no light-induced bulk drift. The kinetic coefficient $G_2^{(2)} > 0$, which determines the bulk component of the buffer gas flow, behaves in a similar manner in collisions between molecules, consistent with the momentum conservation law.

The dependence of the LID on the gas pressure in a capillary obtained in this study is in qualitative agreement with the experimental data of Ref. 7. Unfortunately, it is technically difficult to quantitatively compare theory with experiment⁷ because of the lack of initial data. The basic difficulty of such a comparison, however, has to do with the fact that the theoretical model is based on the assumption that the radiative decay rate of an excited level Γ_m is low compared with the elastic collision rate γ_i . In other words, the dimensionless parameter $\Gamma_{mi} = \Gamma_m / \gamma_i \ll 1$, a condition which is usually satisfied for molecular gas. Under experimental conditions,⁷ the parameter Γ_{mi} increases from 0.3 at high pressures to 140 at low pressures.

The research described in this paper was made possible in part by Grant No. RG4000 from the International Science Foundation.

¹F. Kh. Gel'mukhanov and A. M. Shalagin, JETP Lett. **29**, 711 (1979).

²A. M. Dykhne and A. N. Starostin, Zh. Eksp. Teor. Fiz. **79**, 1211 (1980) [Sov. Phys. JETP **52**, 612 (1980)].

- ³A. V. Ghiner, M. I. Stockmann, and M. A. Vaksman, *Phys. Lett.* **96A**, 79 (1983).
- ⁴M. A. Vaksman and A. V. Ghiner, *Zh. Eksp. Teor. Fiz.* **89**, 41 (1985) [*Sov. Phys. JETP* **62**, 23 (1985)].
- ⁵I. V. Chermnyaninov and V. G. Chernyak, *Inzh. Fiz. Zh.* **55**, 906 (1988).
- ⁶V. G. Chernyak, E. A. Vintovkina, and I. V. Chermnyaninov, *Zh. Eksp. Teor. Fiz.* **103**, 151 (1993) [*JETP* **76**, 82 (1993)].
- ⁷S. N. Atutov, I. M. Ermolaev, and A. M. Shalagin, *Zh. Eksp. Teor. Fiz.* **92**, 1215 (1987) [*Sov. Phys. JETP* **65**, 679 (1987)].
- ⁸S. G. Rautian, G. I. Smirnov, and A. M. Shalagin, *Nonlinear Resonances in Atomic and Molecular Spectra* [in Russian], Novosibirsk, Nauka (1979), p. 310.
- ⁹F. Kh. Gel'mukhanov and A. M. Shalagin, *Zh. Eksp. Teor. Fiz.* **77**, 461 (1979) [*Sov. Phys. JETP* **50**, 234 (1979)].
- ¹⁰F. J. McCormack, *Phys. Fluids* **16**, 2095 (1979).
- ¹¹B. D. Fried and S. D. Conte, *The Plasma Dispersion Function*, Academic Press, New York (1961).
- ¹²V. G. Chernyak, B. T. Porodnov, and P. E. Suetin, *Zh. Eksp. Teor. Fiz.* **43**, 2420 (1973) [*sic*].
- ¹³S. G. Mikhlin, *Variational Methods in Mathematical Physics* [in Russian], Nauka, Moscow (1970), p. 512.

Translated by S. J. Amoretty